

## On the interaction of shock and detonation waves in the TATB-based explosive EDC35

Roberta N. Mulford<sup>a</sup> and Damian C. Swift

*Los Alamos National Laboratory, NM 87545, USA*

Alan M. Collyer and Stephen J. White

*AWE Aldermaston, Reading RG7 4PR, UK*

### Abstract

We have investigated experiments on the TATB-based explosive EDC35, in which a shock wave interacts with a fully-developed detonation wave. The interaction was recorded with an optical framing camera, observing the surface of the explosive through a tamping window. A shock of about 1.5 GPa quenched the detonation from propagating into the preshocked material. The detonation wave became a strong shock, which eventually started to run to detonation once it encountered material which was re-expanding. We were able to reproduce some aspects of this behavior using a temperature-dependent mesoscale reactive flow model, though further work on plasticity terms was clearly needed to obtain proper agreement. The model was calibrated using spectroscopic and shock response data on the constituents of the explosive, and included thermochemical predictions of the equation of state of the detonation products.

### Introduction

Weak shock waves can precondition a chemical explosive, changing the characteristics for initiation of detonation by a second shock. Such behavior has been investigated in a variety of ways. Gas-gun experiments have demonstrated desensitization during the shock-to-detonation transition in chemical explosives [1]. The spatial profile of a fully-developed detonation wave can be perturbed if adjacent material has a higher sound speed, so a shock wave runs ahead in the inert [2]. Complicated loading scenarios like these are fertile ground for testing reactive flow models, as they require greater physical fidelity than does single-shock initiation. Shock desensitization can be explained using reactive flow models which include a representation of the microstructure (in particular, initial porosity) and which invoke a temperature-dependent reaction rate [3].

A more extreme case is the collision between a shock wave and a fully-developed detonation wave. Here, there is a much higher energy density available in the detonation zone compared with the second shock in a double-shock initiation scenario, so one might expect the detonation wave to be fairly insensitive to variations in the state of the material into which it propagates. Shock waves have even been observed to “quench” a detonation wave [4]. Quenching is a particularly valuable test of reactive flow, because it appears to contradict the “chemical spike” theory of detonation [5], which suggests that the leading shock of a detonation wave is sufficiently strong that the explosive loses all memory of its microstructure.

Explosives based on the compound 1,3,5-tri-amino 2,4,6-tri-nitro benzene (TATB) are very insensitive to shock loading. They are known to exhibit interesting phenomena such as dead zones when a detonation wave reaches a sharp corner, and relatively strong dependence of detonation speed on the curvature of the wave. Several years ago, we thought it would be instructive to investigate the interaction between shock and detonation waves in a TATB-based explosive, to see whether the results might guide the design of reactive flow models intended for simulations of shock desensitization.

### Experiments on the shock/detonation interaction

Experiments were performed to study a shock running in a similar direction to a detonation wave, compared with a head-on collision. The experiments used blocks of the explosive EDC35, which consists of 95% by weight TATB and 5% Kel-F binder,  $((C_2F_3Cl)_3C_2H_2F_2)_n$ , with a typical porosity of 2%. The blocks measured 200 mm long by 75 mm high by 23 mm deep. The large faces were enclosed with polymethyl-methacrylate (PMMA) sheets 100 mm thick. One face was marked with a pattern of rectangles of about 20 by 15 mm, drawn onto the surface of the explosive with a black marker pen. During the experiment, this face was illuminated with an argon flash lamp and observed

---

<sup>a</sup>e-mail: mulford@lanl.gov

using a framing camera, taking images  $1 \mu\text{s}$  apart. A preshock of  $\sim 1.5 \text{ GPa}$  was induced using a layer of the plastic explosive PE4 against the long perpendicular face with a PMMA attenuator 3 mm thick. The PE4 was initiated level with the end of the EDC35 block using a track plate lineator. A well-supported detonation wave was induced in the block using a second lineator and a booster charge of UK Composition-B. Experiments were performed with the EDC35 initiated on the surface closest to the preshock initiator so that the directions of propagation of the shock and detonation were generally less than  $90^\circ$  apart (“parallel”), and on the opposite surface so that the shock and detonation collided close to head on (“normal”). Initiation of the EDC35 was delayed with respect to initiation of the PE4, to allow a reasonable amount of explosive to be preshocked before encountering the detonation wave. The depth of the explosive block was the smallest dimension so strictly the flow was three-dimensional; however, the PMMA enclosure acted as a tamper so that surface observations were expected to be quite representative of the bulk behavior. The experiments were fired as shots IS1 (parallel) and IS2 (normal) at AWE Aldermaston, in 1994. (Fig. 1.)

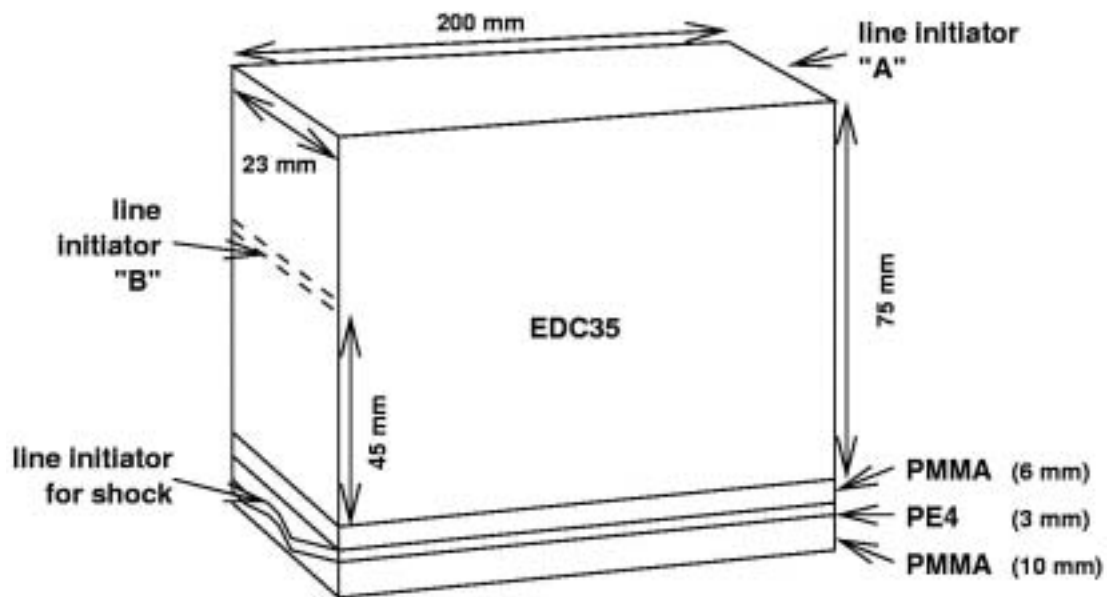


Figure 1: Schematic of EDC35 shock quenching experiments IS1 and IS2.

In both experiments, the shock wave could be seen as a perturbation to the pattern of squares on the surface of the EDC35. The detonation was obvious as a region where the yellow color of the explosive became black and the squares disappeared. Interestingly, small regions of unreacted explosive were left close to the Composition B booster, suggesting that a minor corner turning problem was encountered. These unreacted regions persisted throughout the period covered by the framing camera records. In both experiments, the detonation reactions stopped when the wave encountered preshocked material, and continued as a strong but apparently unreactive shock. A close examination of the interaction point in the parallel case suggests that the detonation stopped after about  $0.2 \mu\text{s}$  or 1 mm; this “time to desensitize” effect has also been observed on other explosives [3]. In the case of parallel interaction (Fig. 2), the desensitized material appeared to be purple over a region a few millimeters wide adjacent to the fully-detonated material; this is suggestive of nitrogen radicals which are likely to be involved in the decomposition of TATB. A localized purple region also appeared after the strong shock had propagated some distance into the preshocked material and was most intense closest to the shock; the framing camera record did not extend long enough to see whether this apparent restarting of reactions eventually ran to detonation. In the case of normal interaction (Fig. 3), the strong shock appeared to be accompanied by reactions after it had propagated roughly 10 mm into the preshocked material, again growing most quickly at the shock, which suggests a heterogeneous reaction mechanism. In the case of normal incidence, the strong shock ran into material which was re-expanding; the growth toward detonation suggests that voids were probably re-opening. In both cases, no unreacted explosive could be seen in the bomb chamber after the experiment. However, most of the charge detonated, and it is likely that in the IS geometry the desensitized material would be consumed after experiencing shock reverberations or in the late-time fireball.

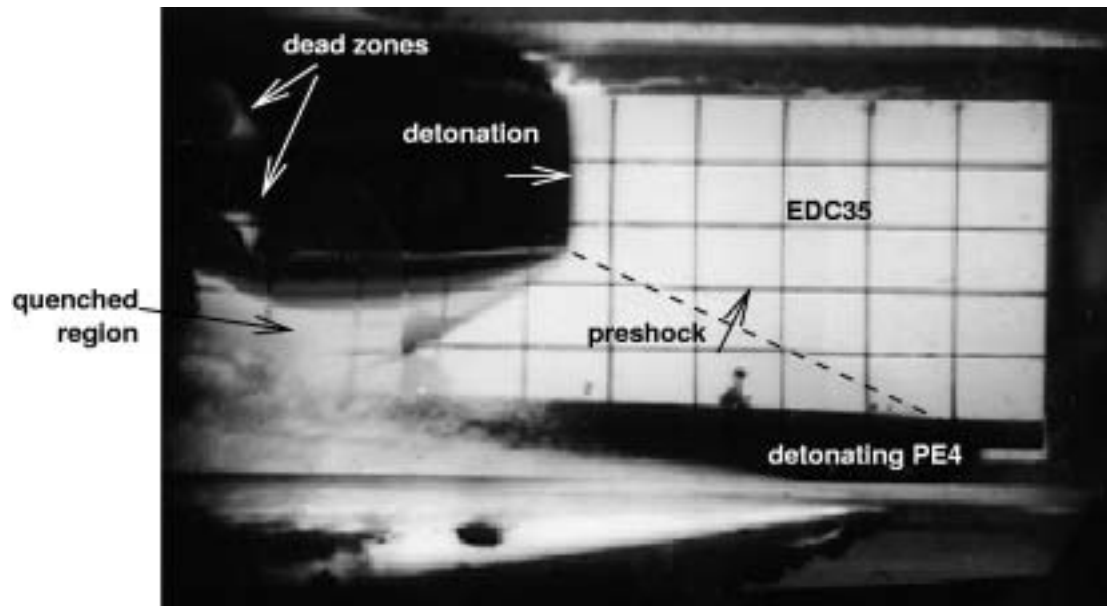


Figure 2: Example framing camera image from parallel interaction between shock and detonation waves (shot IS1).

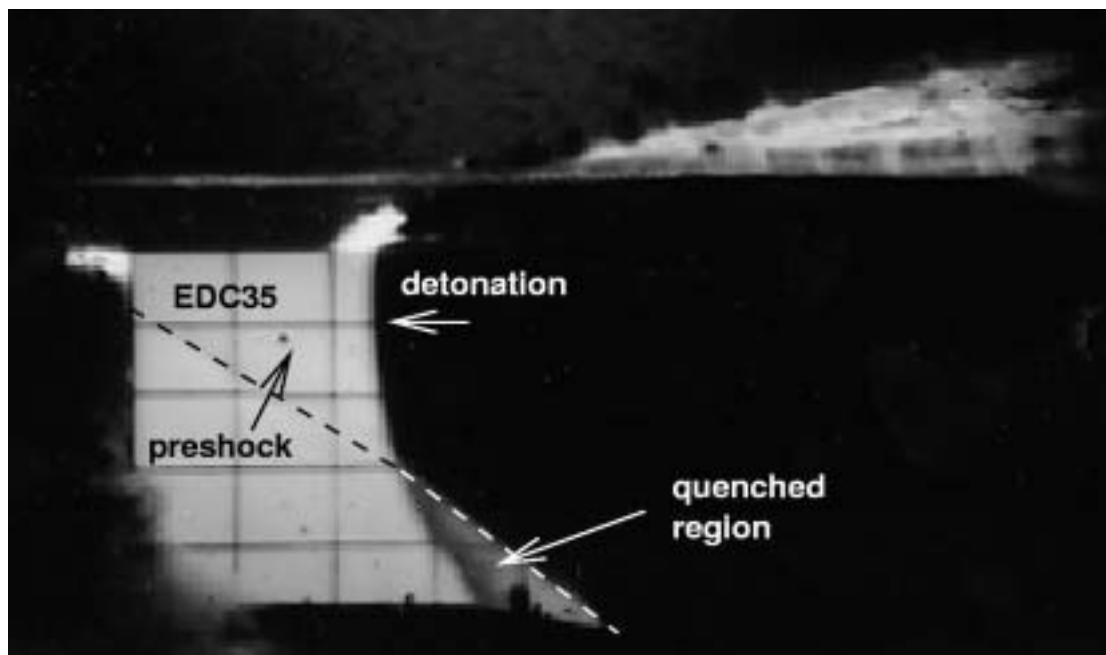


Figure 3: Example framing camera image from normal interaction between shock and detonation waves (shot IS2).

The properties of a fully-developed detonation wave are remarkably insensitive to microstructure. The “chemical spike” model of shock-induced reactions [5] contends that the leading shock of a detonation wave is strong enough to cause extensive chemical reactions in the bulk material, without requiring energy localization at heterogeneities. A preshock of 1.5 GPa is probably strong enough to close most voids, and to cause some compression of the bulk material. The impedance mismatch with virgin material alters the state at the leading shock when the detonation wave collides with the preshock. We estimated the change in pressure and temperature for normal collision by calculating shock Hugoniot, using a Tarver-type Jones-Wilkins-Lee equation of state (EOS) for unreacted LX-17 explosive [6]. LX-17 contains slightly more Kel-F (7.5%) than EDC35 and PBX-9502, but the observed shock Hugoniot is close enough to that of PBX-9502 for the EOS to be valid for this purpose. According to this EOS, the von Neumann spike state at the head of the detonation wave is 2.77 g/cm<sup>3</sup>, 36.2 GPa, and

1679 K and the preshock generates a temperature rise of 29 K from STP. After normal collision, the shock state transmitted into the preshocked material is 2.86 g/cm<sup>3</sup>, 44.9 GPa, and 1456 K; a shock of the same pressure and 1725 K is reflected into the detonation zone. For comparison, the pressure on the principal Hugoniot corresponding to 1456 K is 31.8 GPa. In terms of pressure and compression, the state induced in the preshocked explosive is more extreme than at the von Neumann spike, so reaction rates based on the bulk mechanical state would not predict desensitization. The preshocked material remains cooler than the von Neumann state, so reaction rates based on the bulk temperature may predict desensitization if the reactions are sensitive enough; however, the temperature (and equivalent pressure) and still quite extreme, so one might still expect the shock in the preshocked material to run to detonation in a short distance. More detailed analysis is desirable, using reactive flow models which include a representation of the microstructure.

### **Reactive flow model for EDC35**

A reactive flow model was developed for EDC35, based on our earlier work on nitromethane, HMX, and ammonium nitrate based explosives [4,7,8]. Heterogeneous explosive is treated as a mixture of pure components, each with its own EOS and constitutive model. Porous materials are modeled using the appropriate volume fraction of void or gas. For convenience, we commonly use reaction products in the STP state; the mass density is similar to that of air. Under dynamic loading, the stress state and temperature in each component are allowed to relax exponentially toward the average. An estimate is made of the increased heating caused by localized deformation (plastic strain or viscous flow) close to heterogeneities. Reactions transfer material from one component to another using an Arrhenius rate in which the frequency factor and energy barrier may depend on temperature and pressure. A single rate law is specified for each component of the explosive, though three rates are considered: bulk, bulk pressure but temperature enhanced by localized deformation, and temperature and pressure defined by adjacent material. The last two terms represent hotspots. For EDC35, we first devised new, thermodynamically consistent EOS for TATB, Kel-F, and reaction products of different mixtures of the reactants. We then calibrated the reaction rate for pure TATB against run distances for shock initiation of detonation, for material of a range of porosity. Next we predicted the run distances for PBX-9502, adjusting the microstructural terms slightly to improve agreement. The reactive flow model for EDC35 was the same as that for PBX-9502, except with a smaller initial porosity.

As in our studies on other explosives, we devised a quasiharmonic EOS for each component. However, a new method was followed for EDC35, applied to each solid component in turn. A Grueneisen EOS was fitted to shock Hugoniot data [9], using a simple “snowplow” model to account for data of different initial porosity and discarding data at pressures below the discontinuity in gradient which has been attributed to a phase transition. The Grueneisen EOS was used to estimate the zero Kelvin isotherm, which was then approximated using a Murnaghan fit. The structure of the molecule and/or spectroscopic data were used to estimate the vibrational modes of the material. Each mode was assumed to vary with mass density  $\rho^{1/3}$ , allowing the population of each mode to be predicted as a function of compression and temperature. A thermodynamically complete EOS was constructed in tabular form. The parameters in the Murnaghan fit were adjusted to reproduce the STP state more accurately, and hence to calculate a revised EOS.

For TATB, the shock speed – particle speed data exhibit a discontinuity in gradient which has been attributed to a phase transition. Data at lower pressures were discarded when fitting the Grueneisen EOS. The resulting quasiharmonic EOS also exhibited a degree of curvature; combined with the effect of porous compaction, it was possible to match low pressure data without invoking a phase transition. The agreement was also good at higher pressures. For Kel-F, the quasiharmonic EOS reproduced the shock speed data up to pressures of ~30 GPa, after which the EOS appeared to be too soft. This is likely to reflect inadequacies in the Murnaghan equation. The experimental data for Kel-F extended to higher pressures than did those for TATB.

Thermodynamically complete EOS were calculated for the reaction products of TATB, Kel-F, and mixtures of the two, using the thermochemical computer program CHEETAH [10]. These calculations used exponential-6 potentials between the different species. States were calculated over a rectangular grid in density-temperature space. Densities ranged from 0.01 g/cm<sup>3</sup> to 1.0 g/cm<sup>3</sup> at intervals of 0.01 g/cm<sup>3</sup>, then to 5.0 g/cm<sup>3</sup> at intervals of 0.1 g/cm<sup>3</sup>. Temperatures ranged from 200 to 8500 K at intervals of 100 K. Tables were calculated with Kel-F in the proportions 0, 1, 2, 3, 4, 5, 6, 7, 8, 9, 10, 25, 50, 75, and 100% by mass. Numerical difficulties were encountered in the thermochemical

calculations, particularly at lower temperatures and when Kel-F was included. Missing states were filled in by extrapolation along isochores.

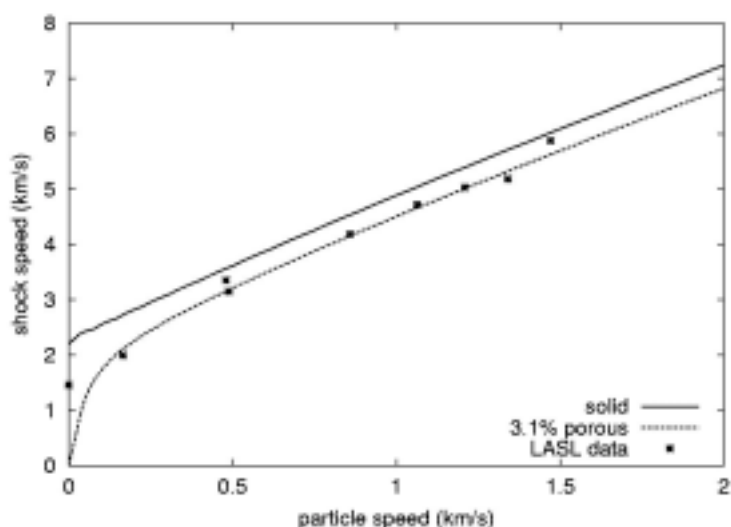


Figure 4: Shock Hugoniot for TATB model, compared with experimental data for 3.1% porous material. Porous calculation used “snowplow” model which is not valid at zero pressure.

The heterogeneous reaction model was similar to that developed previously for HMX-based explosives [4]. The mechanical and thermal equilibration times were estimated using a typical grain size to be 0.1 and 10  $\mu\text{s}$  respectively. Arrhenius parameters were calculated so as to reproduce the run distance for single shock initiation [11] for pure TATB of the highest density reported, and then tested by predicting the run distance for higher porosity. These simulations were performed using a Lagrangian hydrocode with 0.1 mm cell size. A constant pressure was applied to one boundary to induce the initial shock wave. Starting at that boundary, a region of ten cells was included in which the reaction rate was set to zero, in order to mitigate “wall heating” effects which can cause detonation to occur prematurely. This region was not counted as part of the run distance.

Considering the run distance for a single applied pressure, a family of pairs of Arrhenius parameters could be found to reproduce the experimental data, the frequency factor  $Z$  increasing with barrier energy (expressed as a temperature  $T^*$ ). The correct pair of parameters was then chosen by matching the variation of run distance with pressure. Interestingly, for TATB modeled with hotspot heating from gas inclusions but without the plastic enhancement terms, the pressure variation changed little with Arrhenius parameters over many orders of magnitude, and was somewhat steeper than observed experimentally. The uncertainty in the published shock initiation data [11] was sufficiently large that the Arrhenius parameters could not be constrained very closely. Marginally better agreement was obtained for relatively large values of the rate parameters:  $Z = 1.0 \times 10^{13} / \mu\text{s}$ ,  $T^* = 19000 \text{ K}$ . For higher values of the Arrhenius parameters, the model predicted “homogeneous” type shock initiation starting from the surface at which the load was applied, as opposed to “heterogeneous” build up at the shock front.

In this present study, plastic enhancement terms – including a constitutive model – were taken to be the same as were previously developed for HMX [4]: a sensitivity study rather than a rigorous calibration for TATB. Adding the plasticity contribution, the pressure-distance relation varied more with Arrhenius parameters, and better agreement was obtained with the experimental relation, using low values of the parameters:  $Z = 1.0 \times 10^4 / \mu\text{s}$ ,  $T^* = 9000 \text{ K}$  (Fig. 5). This frequency factor is more consistent with values expected for atomic vibrations, but the barrier temperature is in our view implausibly small. For higher values, the relation was again too steep. This is different to the behavior observed for the HMX model, where the plasticity model made it possible to reproduce shock initiation data using significantly higher barrier temperatures, closer to the values inferred from bomb calorimetry experiments on much longer time scales [4]. For TATB, the calorimetry values were  $Z = 3.18 \times 10^{13} / \mu\text{s}$ ,  $T^* = 30157 \text{ K}$  [11]. The variation of the run distance-pressure relation with porosity was reproduced adequately well by the model, again given the relatively large uncertainty in the experimental data (Fig. 6).

Interestingly, some of the TATB simulations exhibited a two-staged build up to detonation. After some distance, the initial shock underwent a transition to a slightly faster speed. This speed persisted over a finite distance, with only relatively gradual acceleration, before a second fairly sharp transition occurred to full detonation. Both transitions were predicted to build up starting near the shock front, and thus presumably reflected heterogeneous phenomena induced by the shock as opposed to long term “cooking” of the bulk material. Micronized and ultra-fine TATB have been observed experimentally to exhibit an “intermediate” region between the initial shock and full detonation, characterized by relatively sharp transition points [11]. These data will be a useful future component in improving the model.

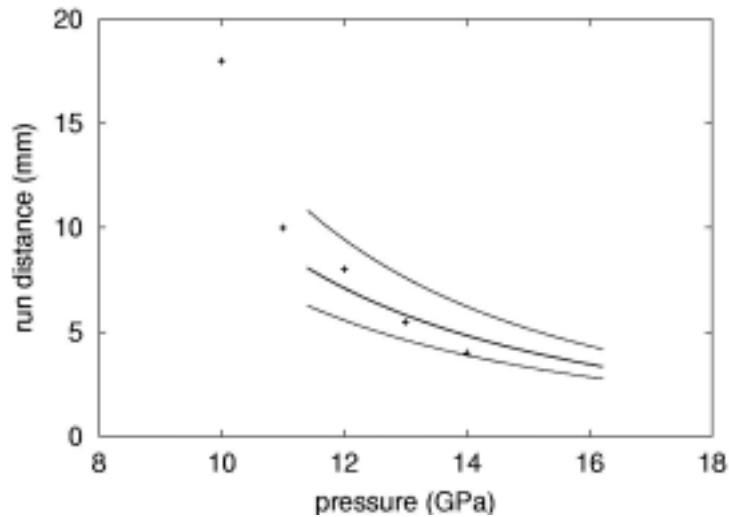


Figure 5: Single-shock run distance for TATB of initial density  $1.876 \text{ g/cm}^3$  (porosity 3.1%). Fit to experimental data (lines, nominal and limits) [11] compared with calculations using temperature-dependent reactive flow model including plasticity terms (points).

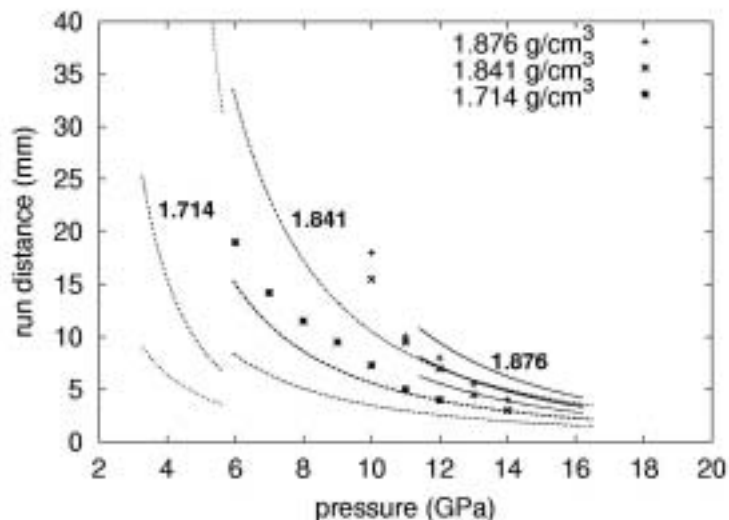


Figure 6: Single-shock run distance for TATB of different initial density. Fit to experimental data (lines, nominal and limits) [11], showing region of validity of data, compared with calculations using temperature-dependent reactive flow model including plasticity terms (points), fitted to data with initial density  $1.876 \text{ g/cm}^3$ .

Calculations were then performed of single shock initiation in PBX-9502. A slow decomposition was included for Kel-F; the run distance was not sensitive to this rate or to the fraction of Kel-F in the gas phase. If the simplistic assumption was used that every component in the heterogeneous mixture shared surface area with every other component, the run distance predicted for PBX-9502 was

systematically too short. PBX-9502 is manufactured by coating the TATB grains with a Kel-F lacquer [11], so TATB is less likely to be exposed directly to hot gas in compressed intergranular pores. The run distance was brought into better agreement – though still slightly more sensitive than the nominal fit to the experimental data – by restricting the surface burn term in the TATB reaction rate to be driven by the state in the Kel-F only (Fig. 7). The reactive flow model used for EDC35 was identical to that for PBX-9502, except with a smaller initial porosity: 2% rather than 6.5%.

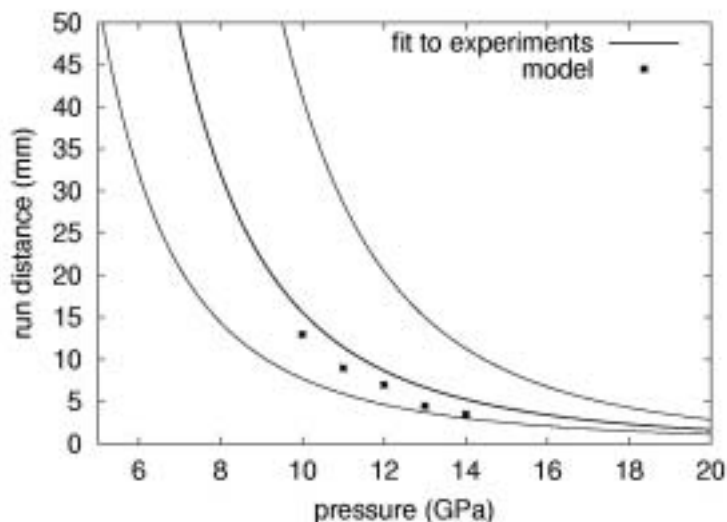


Figure 7: Single-shock run distance for PBX-9502. Fit to experimental data (lines, nominal and limits) [11], compared with calculations using temperature-dependent reactive flow model (points).

#### Predictions of the shock/detonation interaction

Continuum mechanical calculations were made of idealized 1D analogs of the SI experiments. A time-dependent pressure boundary condition was used to induce the 1.5 GPa shock and the detonation wave. The latter was induced by applying a pressure which decreased linearly from 35 GPa to zero over 200 ns. This loading history produced a full-developed detonation wave within 1 to 2 mm. No inert region was included in these simulations, as the 1.5 GPa shock was too weak to induce reactions by wall-heating, and the high pressure portion of the loading history was intended to run to detonation as quickly as possible. Furthermore, the triangular high pressure wave decayed rapidly across the inert region, giving a significantly lower peak pressure when it entered the reactive region, and hence a significantly larger sensitivity to the preshock.

When both waves were induced from the same end (simulating parallel interaction), the reaction rate behind the second shock was suppressed slightly until it caught up with the preshock, for the higher valued Arrhenius parameters used when the plasticity model was omitted. The detonation could not however be said to be quenched. With the plasticity model, no significant suppression of the reaction was predicted. For normal interaction, neither model predicted any desensitization. These results indicate that more development work is needed in the heterogeneous portion of the reactive flow model.

#### Conclusions

The TATB-based explosive EDC35 has been found to exhibit dramatic shock quenching phenomena, in which a shock wave of relatively low amplitude (~1.5 GPa) can extinguish a fully-developed detonation wave. Quenching can occur when the shock runs alongside the detonation, or when the waves collide head-on. The detonation wave drives a strong shock into the pre-shocked region; this shock ultimately shows signs of reaction after running into material which is re-expanding behind the pre-shock.

Simple analysis of the shock interactions shows that the detonation-driven shock induces a higher compression and pressure in the bulk explosive than does the von Neumann spike at the head of the detonation wave, but that the bulk temperature is slightly lower. It may therefore be possible to model shock quenching in EDC35 with a reaction rate based on the bulk temperature, though hotspot effects are more likely to dominate.

We have developed a reactive flow model for TATB-based explosives, using an Arrhenius reaction rate and a representation of the heterogeneous microstructure. The model was calibrated against single shock initiation data for pure TATB, and was capable of predicting the effect on shock initiation properties of variations in porosity and composition. Compared with experimental data, the model was systematically too sensitive to variations in pressure, even when the Arrhenius parameters were altered over a wide range. Simulations of shock initiation did however exhibit a significant “intermediate region” between the essentially inert shock and full detonation, which has been observed experimentally. The model showed some signs of shock desensitization for a detonation wave following an inert shock, though it did not reproduce the quenching effects seen experimentally in EDC35. Future work will focus on improvements to the representation of the microstructure, based on a more recent model of the strength of heterogeneous mixtures, instead of the simplified treatment of strength used in the simulations reported here.

Thermodynamically complete equations of state (EOS) were devised for each component of the heterogeneous mixture: TATB, Kel-F, and reaction products. The EOS for the solid phases used a modified variant of the quasiharmonic scheme we have applied previously to other materials. The EOS for TATB reproduced shock wave data without invoking a phase transition.

### Acknowledgements

We would like to acknowledge the contribution of Paul Selby for helping to perform the experiments, and of Brian Asher, Godfrey Eden, Brian Lambourn, and Ron Winter for useful discussions.

### References

1. R.N. Mulford, S.A. Sheffield and R.R. Alcon, *Initiation of preshocked high explosives PBX-9404, PBX-9502, and PBX-9501, monitored with in-material magnetic gauging*, Proc 10<sup>th</sup> Symposium (International) on Detonation, 1993, ONR 33395-12 (US Office of Naval Research, Washington DC, 1995).
2. G. Eden and R. Belcher, *The effects of inert walls on the velocity of detonation in EDC35, an insensitive high explosive*, Proc 9<sup>th</sup> Symposium (International) on Detonation, held Portland, OR, 1989, OCNR 113291-3 (US Office of Naval Research, Washington DC, 1989).
3. A.W. Campbell (Los Alamos National Laboratory), private communication (1989).
4. R.N. Mulford and D.C. Swift, *Mesoscale modelling of shock initiation in HMX-based high explosives*, Proc 2001 APS Topical Conference on Shock Compression of Condensed Matter, AIP CP620 (AIP, Maryland, 2002).
5. V. Yu. Klimenko, *Multiprocess model of detonation (version 3)*, Proc International Workshop on New Models and Numerical Codes for Shock Wave Processes in Condensed Media, held St Petersburg, Russia, 10-14 July 1995.
6. P.C. Souers and L.C. Haselman Jr, *Detonation equation of state at LLNL*, Lawrence Livermore National Laboratory report UCRL-ID-116113 (1994).
7. R.N. Mulford and D.C. Swift, *A temperature-dependent reactive flow model for nitromethane*, Proc International Workshop on New Models and Hydrocodes for Shock Waves in Condensed Matter, held Edinburgh, Scotland, May 2002 (to appear).
8. R.N. Mulford, M. Braithwaite, and D.C. Swift, *A temperature-dependent reactive flow model for ANFO*, Proc 12<sup>th</sup> International Detonation Symposium, held San Diego, CA, August 2002 (to appear).
9. S.P. Marsh, “LASL Shock Hugoniot Data” (University of California Press, Berkeley, 1980).
10. L.E. Fried, W.M. Howard, P.C. Souers, and P.A. Vitello (Lawrence Livermore National Laboratory), “CHEETAH” version 3.0, software and documentation (2001).
11. T.R. Gibbs and A. Popolato, “LASL Explosive Property Data” (University of California Press, Berkeley, 1980).